2D analysis of polydisperse core-shell nanoparticles using analytical ultracentrifugation

AUTHORS: JOHANNES WALTER, GARY GORBET, TUGCE AKDAS, DORIS SEGETS, BORRIES DEMELER, AND WOLFGANG PEUKERT

PRESENTED BY REECE MARTIN

BCHM5000: HYDRODYNAMIC METHODS

25/3/24

Presentation Topics

- Intro to core-shell nanoparticles (NPs)
- Studying NPs using AUC
- Comparing NP analysis methods
  - Simulated datasets
  - Experimental datasets
    - Zinc Oxide (ZnO) NPs
    - Copper Indium Sulphide ($CuInS_2$) QDs
- Conclusions

What are core-shell nanoparticles (NPs)?

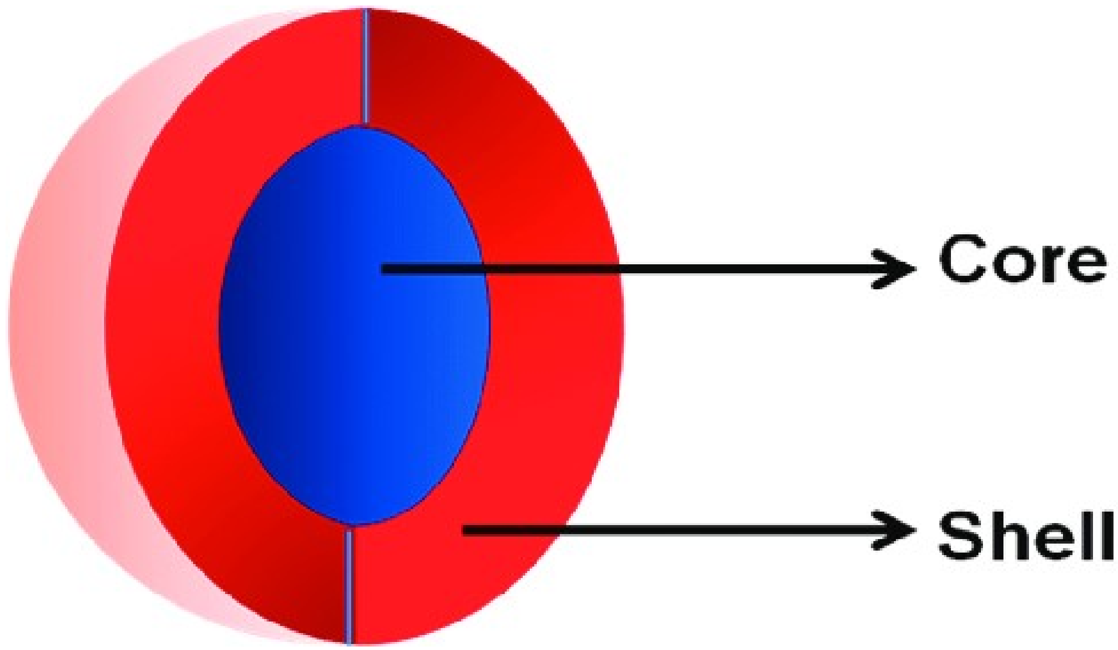

Figure 1. Schematic diagram of a core-shell nanoparticle [3]

Why study core-shell NPs?

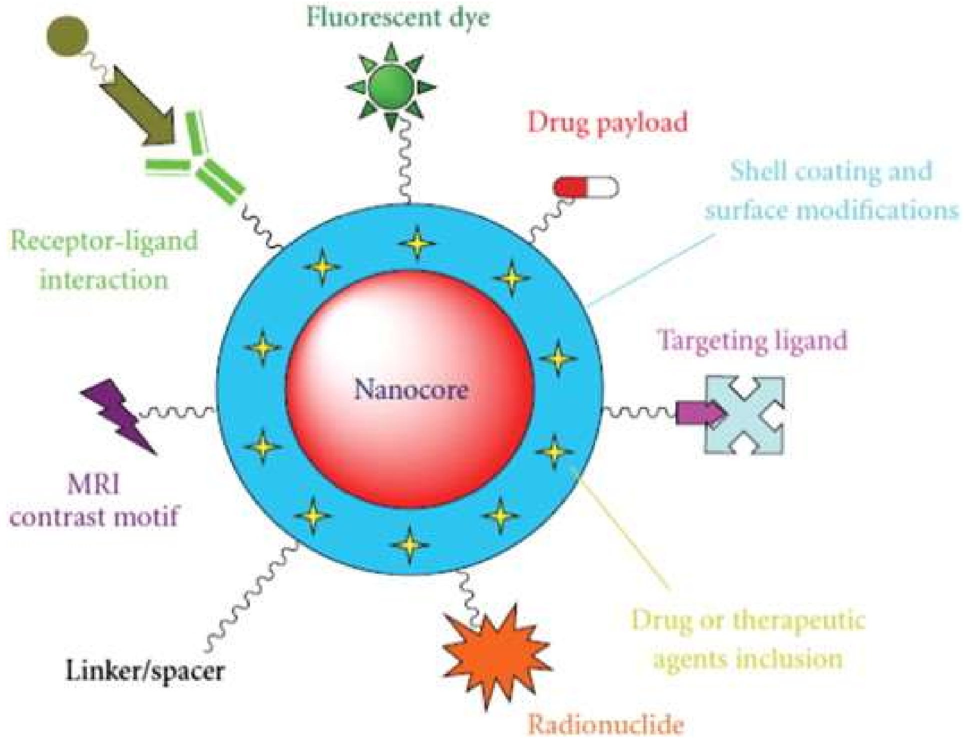

Figure 2. Diagram showing some biomedical applications of core-shell NPs [4]

Why study NPs using AUC?

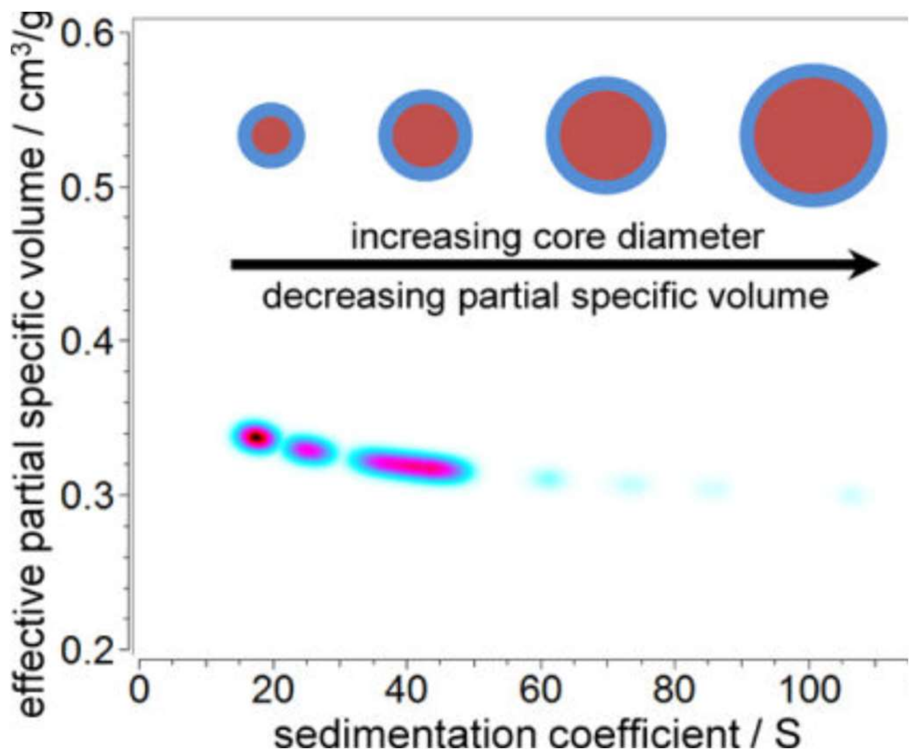

Figure 3. Pseudo-3D distribution of effective partial specific volume and sedimentation coefficient with increasing NP core diameter [1]

Approach to studying NPs using AUC

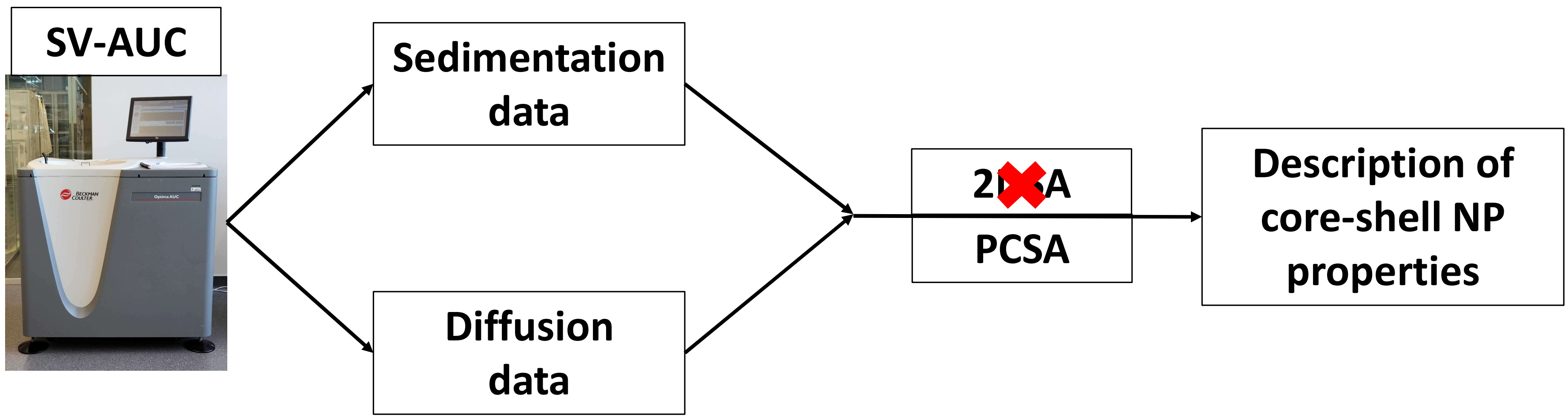

Figure 4. General Workflow for collecting, analyzing and reporting data on polydisperse PSDs

Effects of NP core diameter

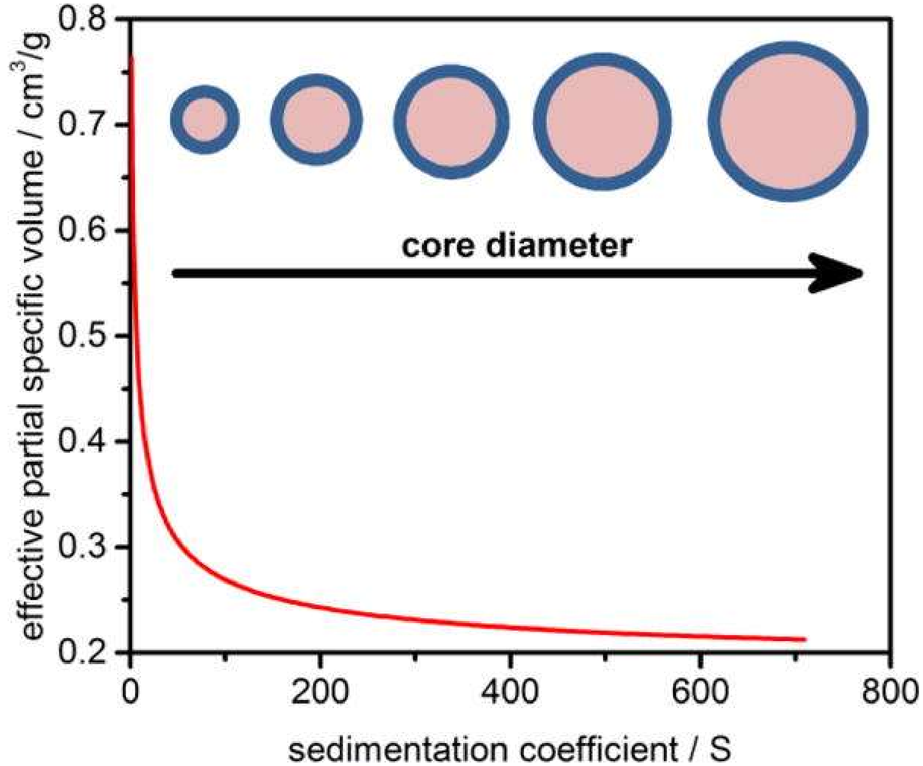

Figure 5. Schematic diagram of the dependence of the effective partial specific volume on increasing sedimentation coefficient [1].

What is effective partial specific volume?

$$\rho_{p,eff} = \frac{1}{\bar{\nu}_{p,eff}} = \frac{18\eta s}{{d_{V,eff}}^2} + \rho_s = \frac{162\pi^2\eta^3 s D^2}{{k_B}^2 T^2} + \rho_s$$

Effective density and partial specific volume equation for a spherical NP, where

$$\frac{f}{f_0} = 1 \quad \rightarrow \quad d_h = d_{V,eff} = d_{p,eff}$$

Accurate $\rho_{p,eff}$ and $\bar{v}_{p,eff}$ determinations require good s, D, and $\frac{f}{f_0}$ information

Core-shell NP properties determination workflow

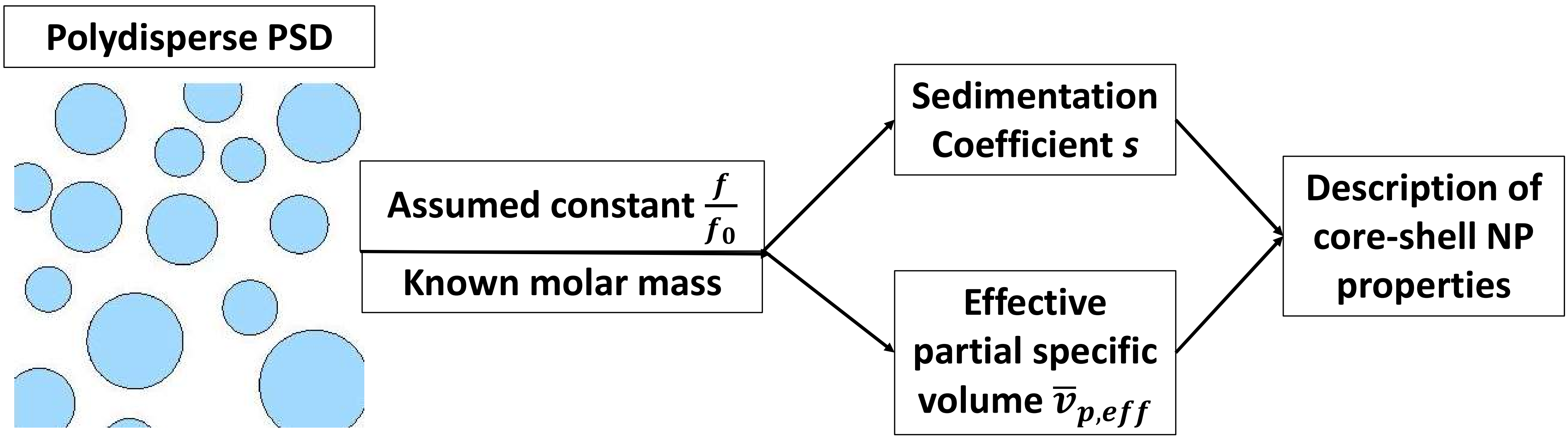

Figure 6. Workflow for describing the core-shell NP properties of a polydisperse PSD [6].

2DSA-CG vs PCSA Analysis Methods

Figure 7. Example of a 2DSA-CG with varying s and $\bar{v}_{p,eff}$, but fixed $\frac{f}{f_0}$

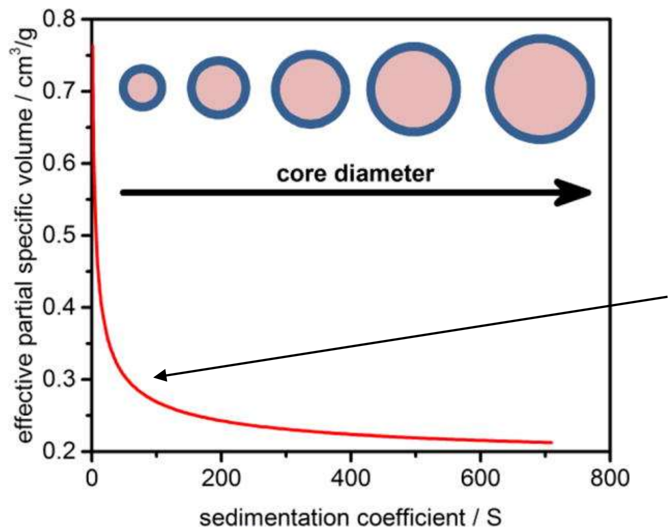

Figure 8. Dependence of effective partial specific volume on sedimentation coefficient [1].

2nd order power law parametrization:

$$\bar{\boldsymbol{v}}_{\boldsymbol{p,eff}} = \boldsymbol{a}\boldsymbol{s}^{\boldsymbol{b}} + \boldsymbol{c}$$

2nd Order Power Law Parametrization

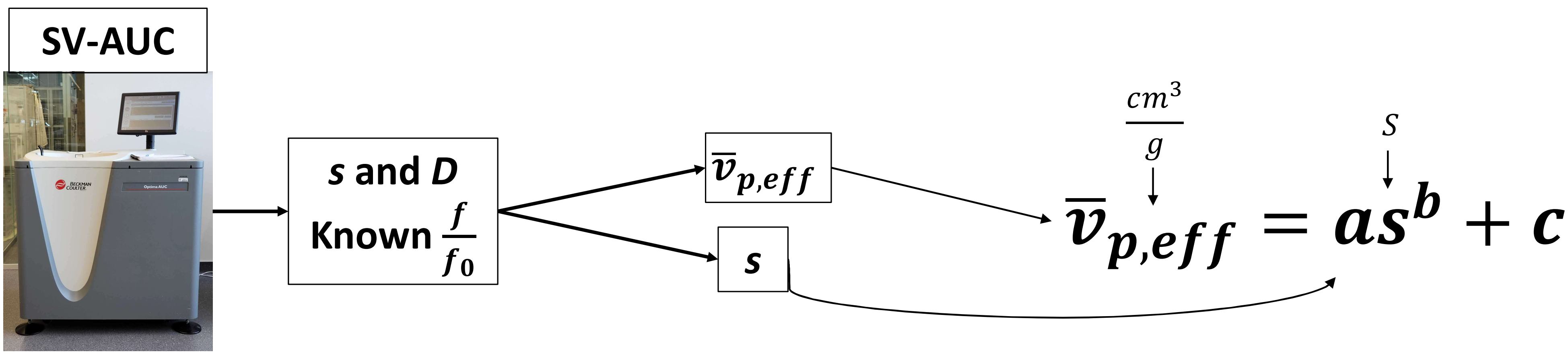

Figure 9. 2nd order power law parametrization workflow for *s* and $\bar{v}_{p,eff}$ [1].

Examples of the 2nd power law parametrization

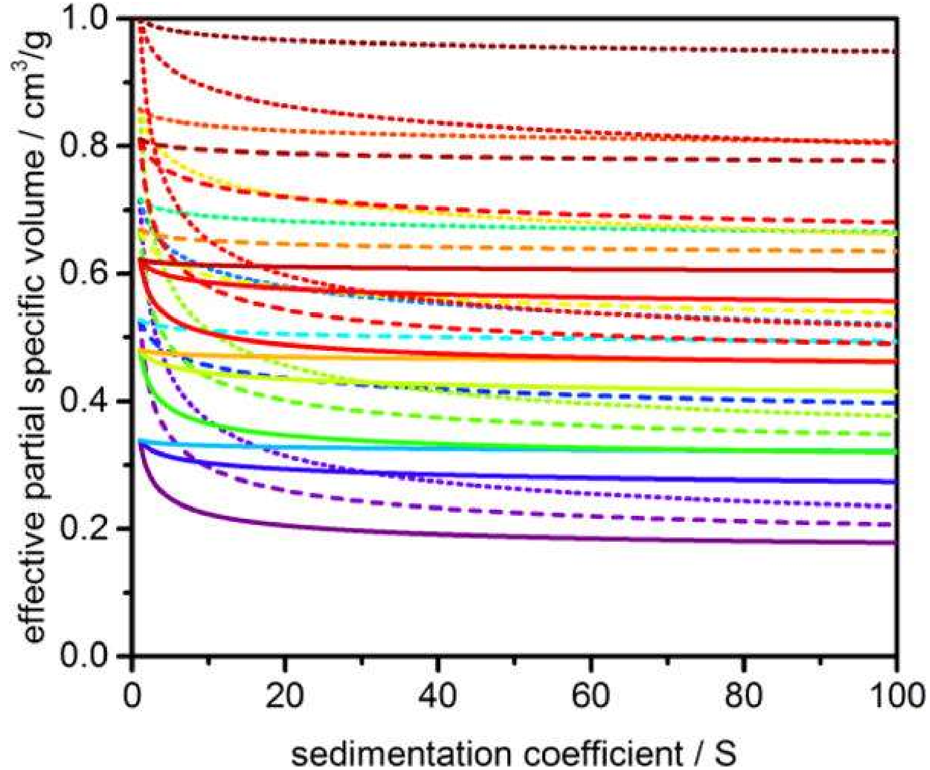

Figure 10. Example curves produced by the 2nd order power law parametrization [1].

Simulated NP Datasets

Model #1: Narrow monomodal PSD

Model #2: Narrow multimodal PSD

Model #3: Multimodal polydisperse PSD

Model #4: Multimodal polydisperse PSD

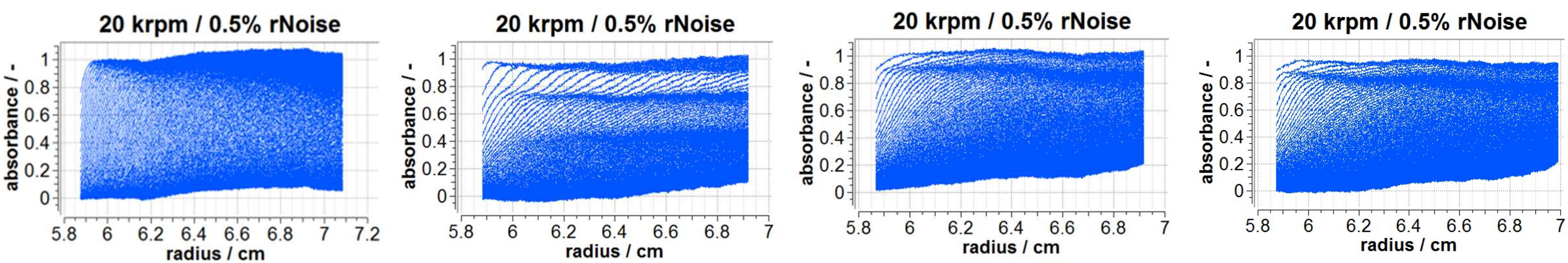

Figure 11. Simulated NP datasets for each model number. Only datasets simulated at 20 krpm and 0.5% random noise were presented for ease of comparison [1].

c(s) Analysis of Simulated NP Datasets

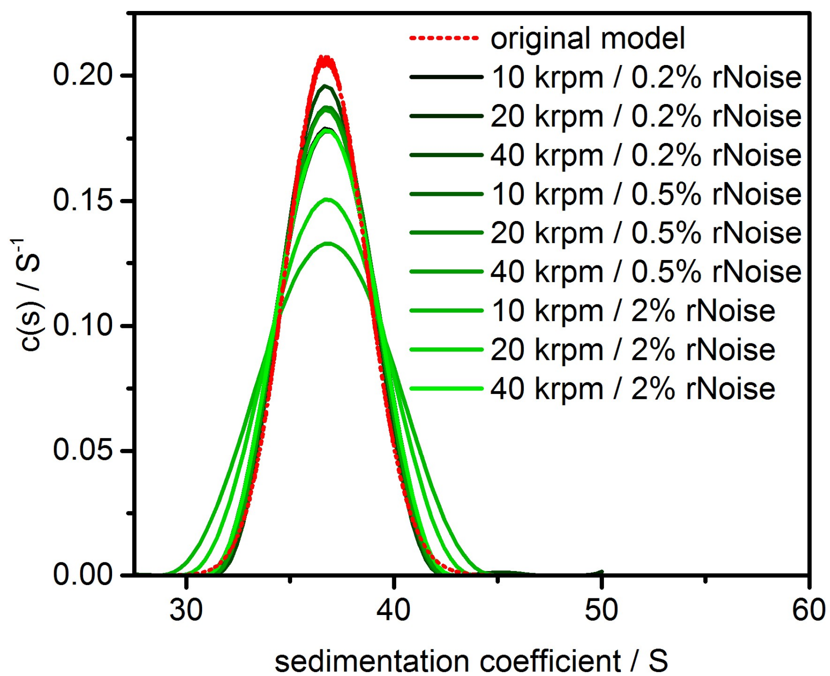

Figure 12. 1D c(s) analysis of the simulated datasets for model #1 (narrow monomodal PSD) [1].

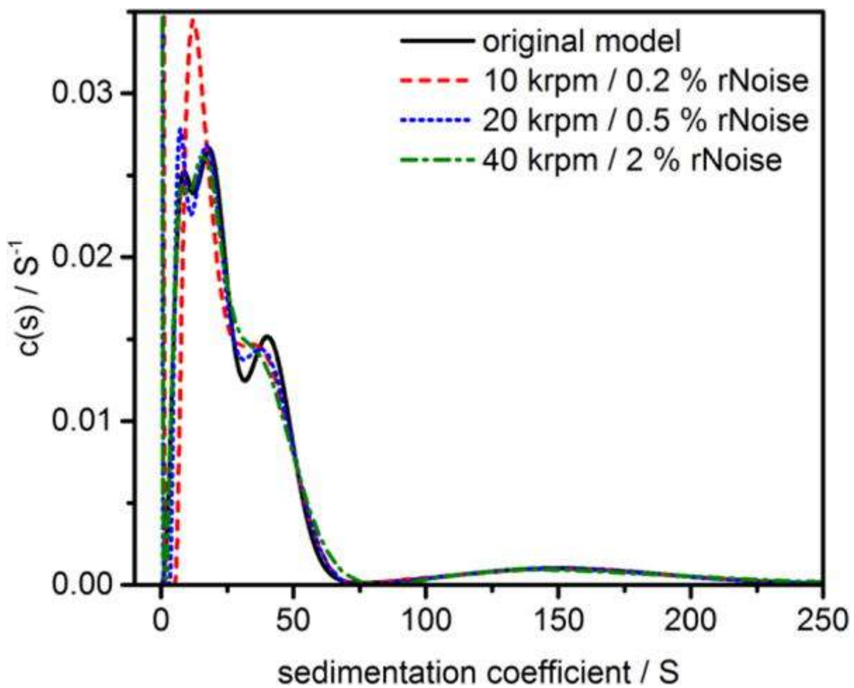

Figure 13. 1D c(s) analysis of the simulated datasets for model #3 (multimodal polydisperse PSD) [1].

c(s,D) Analysis of Simulated NP Datasets

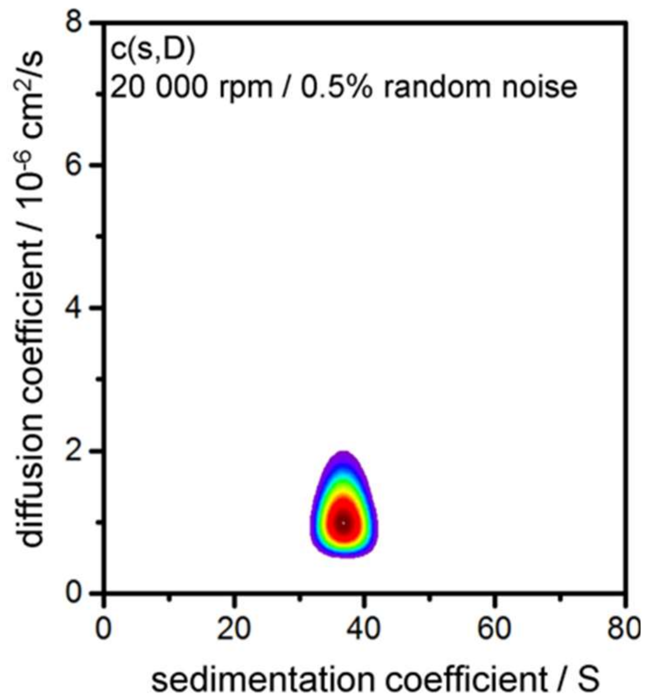

Figure 14. 2D c(s,D) analysis of a simulated dataset for model #1 (narrow monomodal PSD) [1].

2DSA-CG-MC Analysis of Simulated NP Datasets

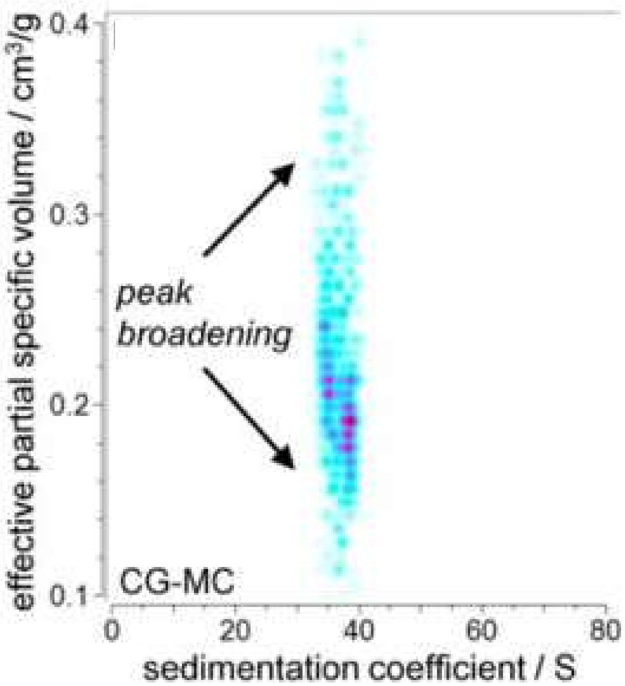

Figure 15. 2DSA-CG-MC analysis of the simulated datasets for model #1 (narrow monomodal PSD) at 40 krpm and 2% random noise [1].

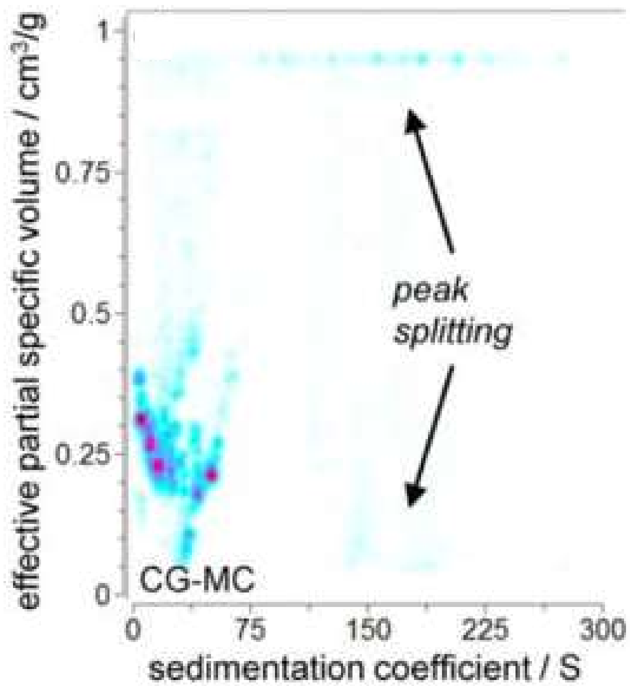

Figure 16. 2DSA-CG-MC analysis of the simulated datasets for model #3 (multimodal polydisperse PSD) at 20 krpm and 0.5% random noise [1].

2DSA-CG-MC vs PCSA-TR for Simulated NP Datasets

$$\bar{v}_{p,eff} = as^b + c$$

2DSA-CG-MC:

$\bar{v}_{p,eff}$ vs. s

100 by 100 grid
=
10000 grid points

Many overlapping solutions

Grid points reduced by a factor of 100

→

2nd order power law PCSA:

$\bar{v}_{p,eff} - s$ parametric curve

100 grid points

Minimal overlapping solutions

PCSA-TR for Simulated NP Datasets

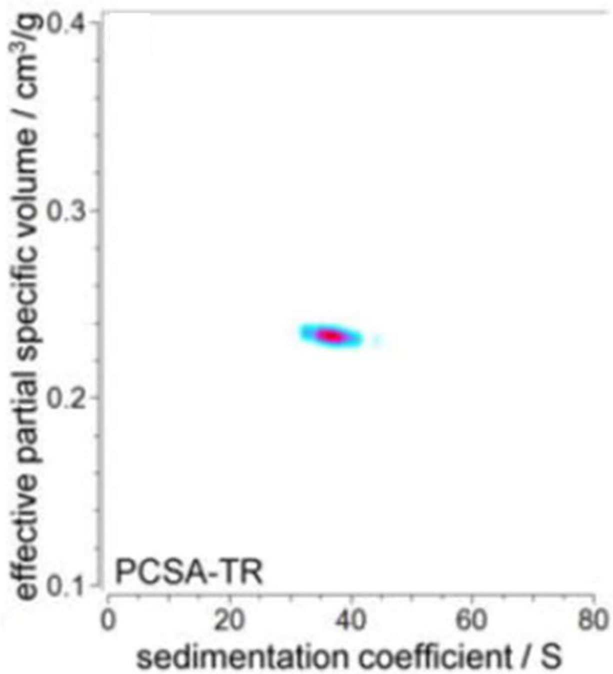

Figure 17. PCSA-TR analysis of the simulated datasets for model #1 (narrow monomodal PSD) at 40 krpm and 2% random noise [1].

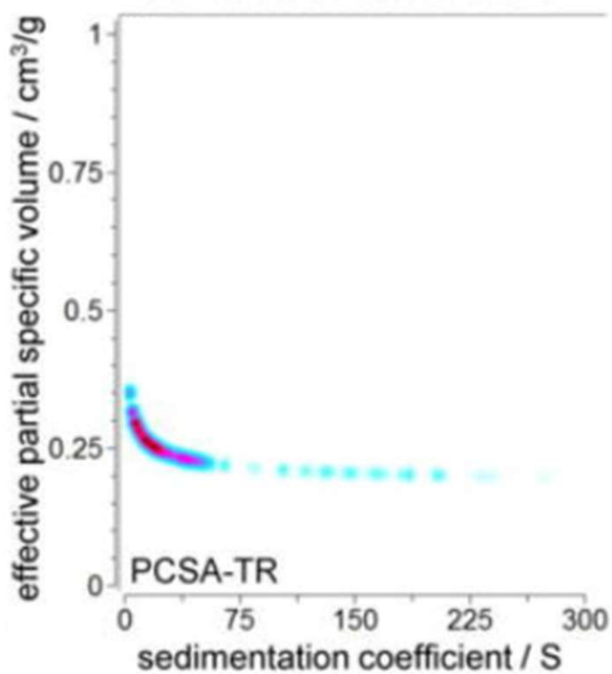

Figure 18. PCSA-TR analysis of the simulated datasets for model #3 (multimodal polydisperse PSD) at 20 krpm and 0.5% random noise [1].

PCSA-TR for Simulated NP Datasets

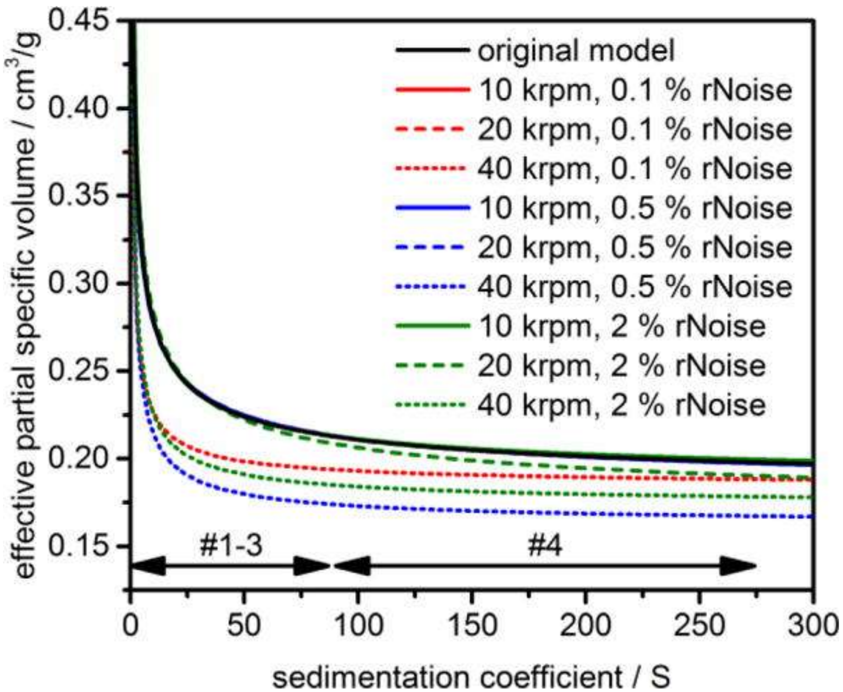

Figure 19. Dependence of $\bar{v}_{p,eff}$ on s in model #3 (multimodal polydisperse PSD), and best fit parametrizations at various rotor speeds and noise levels [1].

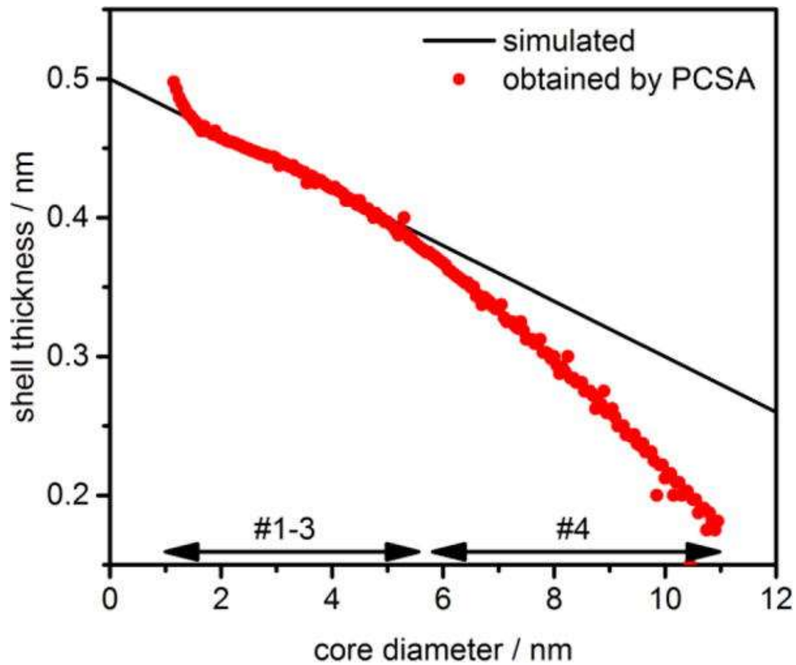

Figure 20. Relationship between shell thickness and core diameter for the simulated data and results of PCS-TR [1].

Experimental NP Dataset Collection

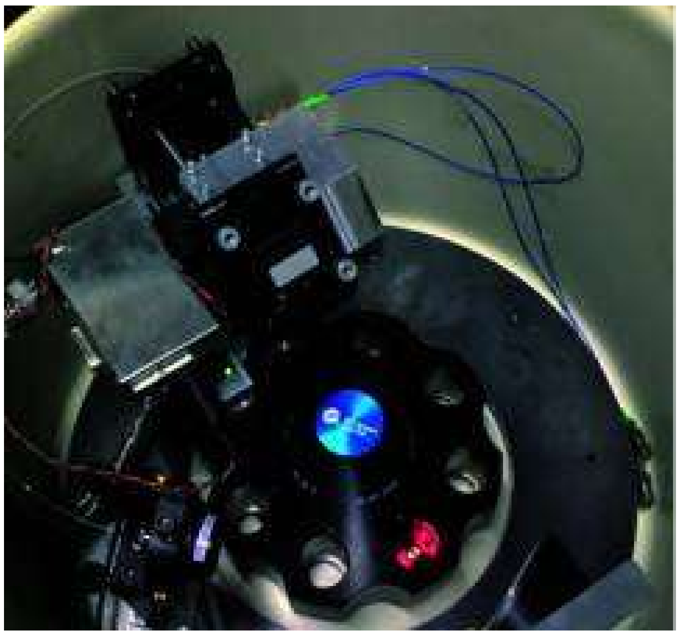

Figure 21. Custom UV/Visible multiwavelength (MWL) detector in a similar setup to the one used by the authors [10].

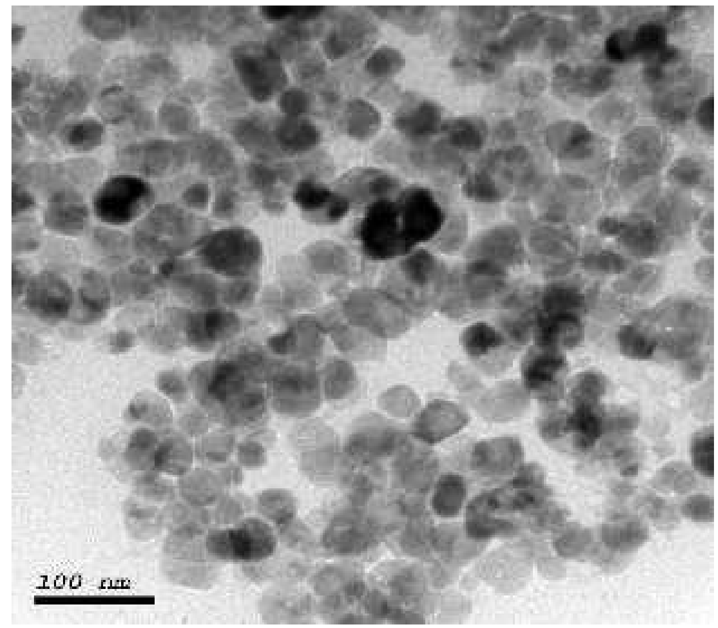

Figure 22. TEM image of nanoparticles similar to those used in this experiment [11].

Zinc Oxide (ZnO) NPs

Figure 23. Computer illustration of Zinc oxide (ZnO) NPs [7]

ZnO NPs Experimental Data

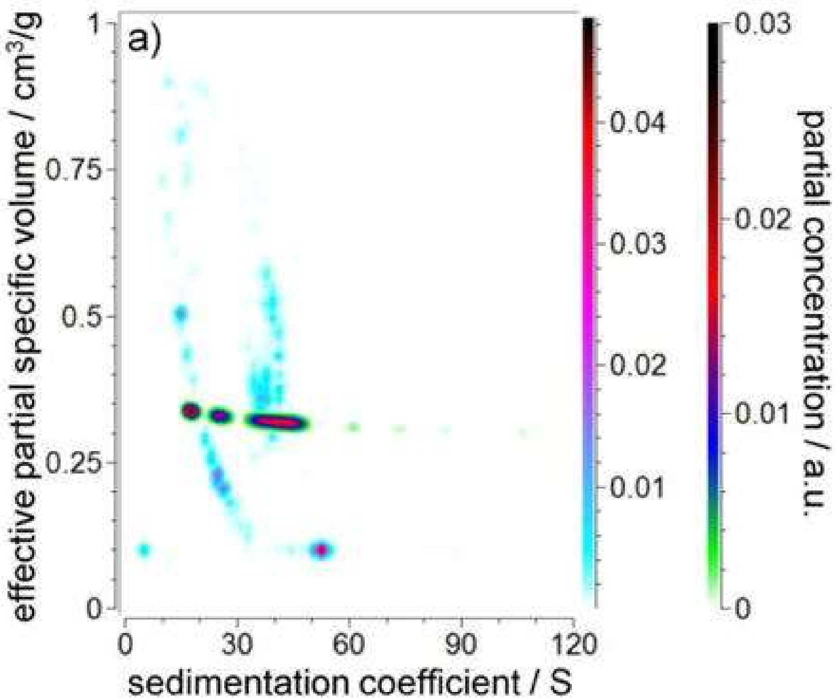

Figure 24. 2DSA-CG-MC (blue-purple-red) and PCSA-TR (green-blue-red) analyses of the ZnO NPs after 3 hr ripening [1].

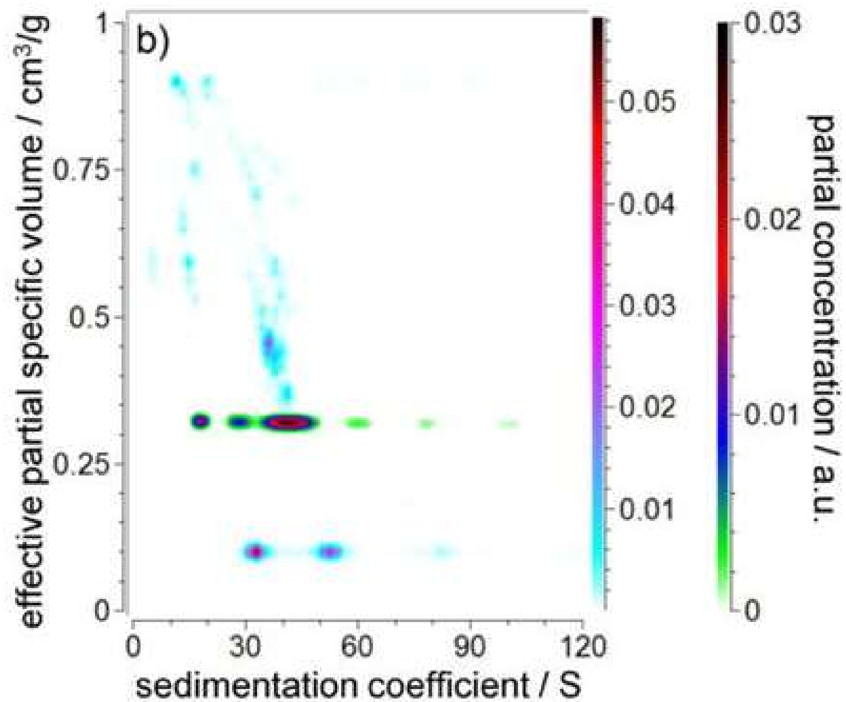

Figure 25. 2DSA-CG-MC (blue-purple-red) and PCSA-TR (green-blue-red) analyses of the ZnO NPs after 4 hr ripening [1].

Copper Indium Sulphide ($CuInS_2$) QDs

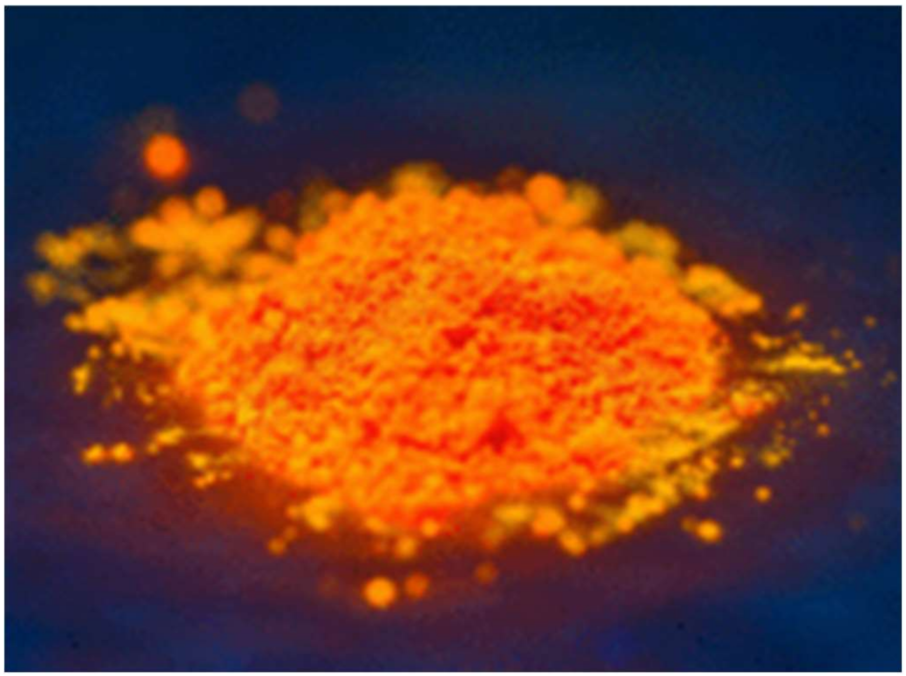

Figure 26. Image of $CuInS_2$ quantum dots with an EM radiation emission peak at about 590nm, which appears orange [8].

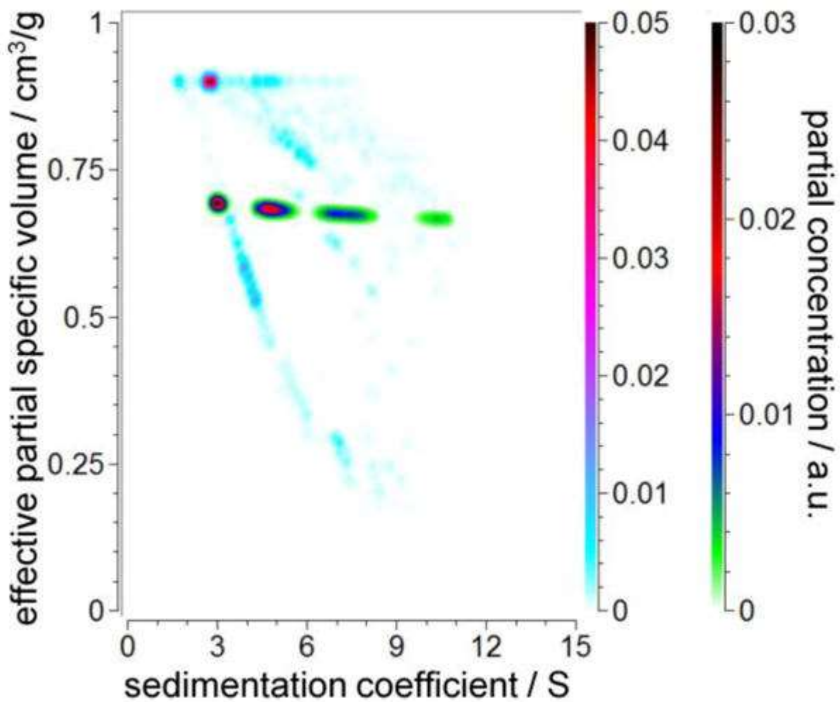

Figure 27. 2DSA-CG-MC (blue-purple-red) and PCSA-TR (green-blue-red) analyses of the ZnO NPs after 4 hr ripening [1].

Conclusions

- 1D and 2D analysis methods fail to properly characterize the core-shell properties of polydisperse PSDs due to their improper treatment of $\bar{v}_{p,eff}$.
- The new 2nd order power law PCSA properly characterizes the core-shell properties of polydisperse PSDs both from simulated and experimental data.
- More work needs to be done to accurately characterize PSDs with varying shell thickness.

References

[1] Walter, J., Gorbet, G., Akdas, T., Segets, D., Demeler, B., & Peukert, W. (2016). 2D analysis of polydisperse core-shell nanoparticles using analytical ultracentrifugation. The Analyst, 142(1), 206–217. https://doi.org/10.1039/c6an02236g

[2] Nomoev, A. V., Bardakhanov, S. P., Schreiber, M., Bazarova, D. G., Romanov, N. A., Baldanov, B. B., Radnaev, B. R., & Syzrantsev, V. V. (2015). Structure and mechanism of the formation of core-shell nanoparticles obtained through a one-step gas-phase synthesis by electron beam evaporation. Beilstein journal of nanotechnology, 6, 874–880. https://doi.org/10.3762/bjnano.6.89

[3] Patra, A. Core–Shell (CS) Nanostructures and Their Application Based on Magnetic and Optical Properties - Scientific Figure on ResearchGate. Available from: https://www.researchgate.net/figure/Schematic-diagram-of-core-shell-nanostructure_fig1_272274390

[4] Krishnendu Chatterjee, Sreerupa Sarkar, K. Jagajjanani Rao, Santanu Paria, Core/shell nanoparticles in biomedical applications, Advances in Colloid and Interface Science, Volume 209, 2014, Pages 8-39, ISSN 0001-8686, https://doi.org/10.1016/j.cis.2013.12.008.

[5] Chaudhuri, R. G. & Paria, S. Core/Shell Nanoparticles: Classes, Properties, Synthesis Mechanisms, Characterization, and Applications. Chemical Reviews 2012 112 (4), 2373-2433. DOI: 10.1021/cr100449n

[6] Borkovec, M. Size and mass distributions of particles and polymers. Laboratory of Colloid and Surface Chemistry (LCSC). https://colloid.ch/index.php?name=distributions

[7] AZoNano. (2019, September 17). Zinc oxide (ZnO) nanoparticles – Properties & Applications. https://www.azonano.com/article.aspx?ArticleID=3348

[8 Strem Chemicals. Copper Indium Disulfide Quantum Dots. 927198-36-5. (n.d.). https://www.strem.com/catalog/v/29-8510/17/copper_927198-36-5

[9] Science Direct. Quantum Dots – An Overview. https://www.sciencedirect.com/topics/earth-and-planetary-sciences/quantum-dot

[10] Wawra, S. E., Onishchukov, G., Maranska, M., Eigler, S., Walter, J., & Peukert, W. (2019). A multiwavelength emission detector for analytical ultracentrifugation. Nanoscale advances, 1(11), 4422–4432. https://doi.org/10.1039/c9na00487d

[11] ResearchGate. Studying the Antimicrobial Effect of Nanoparticles on different Microbial Clinical Isolates. Available from: https://www.researchgate.net/figure/TEM-image-of-ZnO-NPs-showed-nearly-spherical-nanoparticles-with-average-50-nm_fig5_327868185